Макрогетероциклы
http://macroheterocycles.isuct.ru

DOI: 10.6060/mhc200500r

Synthesis by the Hummelen–Wudl Method and Physicochemical Study of Pyropheophorbide–Fullerene Dyad

Alexei V. Kozlov,[a] Alexander Yu. Rybkin,[a@] Alexandra Yu. Belik,[a] Kamil R. Taziev,[b,a] Pavel A. Tarakanov,[a,c] Nikolay S. Goryachev,[a,b] Ilya V. Sulimenkov,[d] Viatcheslav I. Kozlovskiy,[d,c] Yulia V. Romanenko,[e] Mikhail O. Koifman,[e] Fedor E. Gostev,[f] Ivan V. Shelaev,[f] Arsenii V. Aybush,[f] Viktor A. Nadtochenko,[f] and Alexander I. Kotelnikov[a,b]

[a]*Institute of Problems of Chemical Physics RAS, 142432 Chernogolovka, Russia*
[b]*Lomonosov Moscow State University, 119991 Moscow, Russia*
[c]*Institute of Physiologically Active Compounds RAS, 142432 Chernogolovka, Russia*
[d]*Chernogolovka Branch of the N.N. Semenov Federal Research Center for Chemical Physics, RAS, 142432 Chernogolovka, Russia*
[e]*Ivanovo State University of Chemistry and Technology, 153000 Ivanovo, Russia*
[f]*N.N. Semenov Federal Research Center for Chemical Physics, RAS, 119991 Moscow, Russia*
[@]*Corresponding author E-mail: alryb@icp.ac.ru*

A new type of pyropheophorbide-fullerene[60] dyad was synthesized by their attachment by the cyclopropane backbone at the 13(1)-position of the chlorin macrocycle using the Hummelen-Wudl method. Here we report a complex analysis of the structure influence on the photophysical properties of the newly obtained dyad and its comparison with another pyropheophorbide-fullerene[60] dyad. The latter dyad was previously obtained by the attachment of the tetrahydropyrrole backbone at the third position of the macrocycle using the Prato reaction. It was shown by quantum-chemical modeling that the studied dyads have drastically different spatial positions of the fullerene core relative to the dye macrocycle plane: "parallel" for the former and "perpendicular" – for the latter. The influence of structural differences on various properties of dyads was studied: the aggregation properties, absorption spectra, the fluorescence quenching of the dye moiety in the dyads, and the lifetimes of excited states. The data obtained are important for the further development of methods for the directional design of the photoactive fullerene-dye structures – highly effective photosensitizers for photodynamic therapy.

Keywords: Pyropheophorbide, fullerene derivatives, dyad, synthesis, mass spectrometry, matrix-assisted ionization, fullerene-dye excimers relaxation kinetics, conformation.

Синтез методом Хюммелена–Вудла диады пирофеофорбид–фуллерен и исследование её физико–химических свойств

А. В. Козлов,[a] А. Ю. Рыбкин,[a@] А. Ю. Белик,[a] К. Р. Тазиев,[b,a] П. А. Тараканов,[a,c] Н. С. Горячев,[a,b] И. В. Сулименков,[d] В. И. Козловский,[d,c] Ю. В. Романенко,[e] М. О. Койфман,[e] Ф. Е. Гостев,[f] И. В. Шелаев,[f] А. В. Айбуш,[f] В. А. Надточенко,[f] А. И. Котельников[a,b]

[a]*Институт проблем химической физики РАН, 142432 Черноголовка, Россия*
[b]*Московский государственный университет им. М.В. Ломоносова, 119991 Москва, Россия*
[c]*Институт физиологически активных веществ РАН, 142432 Черноголовка, Россия*
[d]*Филиал Федерального исследовательского центра химической физики им. Н.Н. Семенова РАН в г. Черноголовка, 142432 Черноголовка, Россия*
[e]*Ивановский государственный химико-технологический университет, 153000 Иваново, Россия*
[f]*Федеральный исследовательский центр химической физики им. Н.Н. Семенова РАН, 119991 Москва, Россия*
[@]*E-mail: alryb@icp.ac.ru*

Синтезирован новый тип диады пирофеофорбид-фуллерен[60] путем их сочленения циклопропановым остовом по 13(1)-положению макроцикла с помощью метода Хюммелена-Вудла. На примере новой диады и ранее полученной диады пирофеофорбид-фуллерен[60], сочлененной тетрагидропиррольным остовом по 3 положению макроцикла с помощью реакции Прато, был проведен комплексный анализ влияния их структуры на фотофизические свойства. Квантово-химическое моделирование показало, что исследуемые диады обладают различным пространственным положением ядра фуллерена относительно плоскости макроцикла красителя: «параллельным» для первой диады и «перпендикулярным» – для второй. Исследовано влияние структурных отличий на различные свойства диад: склонность к агрегации, спектры поглощения, степень тушения флуоресценции красителя в составе диад и времена жизни возбужденных состояний. Полученные данные имеют важное значение для дальнейшего развития методов направленного дизайна фотоактивных структур фуллерен-краситель – новых высокоэффективных фотосенсибилизаторов для фотодинамической терапии.

Ключевые слова: Пирофеофорбид, фуллерен, диада, синтез, масс-спектрометрия, матрично-активированная ионизация, кинетика релаксации эксимеров в диадах фуллерен-краситель, конформация.

Introduction

Hybrid structures based on dyes and fullerene C_{60} attract researchers with their unique photophysical and electron-donor properties. They have already found wide applications in the fields of optoelectronics, photovoltaics, sensor design, and many other applications.[1–5] Such fullerene-based structures are of particular interest as photosensitizers (PS) for photodynamic therapy (PDT). When the fullerene goes into the excited state, it can efficiently generate reactive oxygen species (ROS) and cause tumor damage. However, nowadays only a small share of the work on the fullerene-dye structures (so-called "dyads") is devoted to their use in PDT,[6–8] and the urgent task is to find approaches that allow us to obtain the optimal combination of photophysical properties and high photodynamic activity of fullerene-dye dyads.

For the application in PDT, the promising way is the combination of fullerene with the dyes, which have high absorption in the red spectral region. Earlier, we have created a number of fullerene-chlorin dyads, for which a high generation efficiency of superoxide was shown.[9–11] It was also shown that the decrease of linker length between the dye and fullerene core significantly increases the activity of the dyads.[9] The second important point that should be taken into account – is the fact that with each new addend attached to the fullerene core significantly decreases the ROS quantum yield (of both superoxide and singlet oxygen). This effect is caused by the disruption of C_{60} spheroid symmetry, which leads to the increase of both LUMO energy[12–16] and the energy of triplet excited state[17,18] of fullerene.

Thus, to obtain high photodynamic activity of fullerene-dye dyad, two requirements must be met – the shortest linker length between the fullerene core and the dye, and the lowest possible degree of the fullerene core modification. The first step to verify this assumption was our work,[10] where the methods of synthesis and purification were optimized to obtain a fullerene-chlorin dyad, and the efficiency of ROS generation of the dyad was evaluated. For that dyad, it was shown that the efficiency of the singlet oxygen generation dropped while the efficiency of superoxide generation increased by more than 18 times,[10] which was significantly higher than for the previously obtained dyads.[9,11]

Thus, the aim of the present work was to develop approaches to the synthesis of fullerene-chlorin dyads with a short linker and different mutual positions of the π-aromatic systems of the dye and the fullerene core and conduct a comparative analysis of the effect of the dyads structure on their photophysical properties. We selected two structures of fullerene-chlorin dyads that meet the above-listed requirements – the shortest linker length and the lowest possible degree of fullerene core modification. The already known fullerene-methylpyropheophorbide dyad,[19–21] obtained by the Prato reaction, was chosen as the first dyad, and the fullerene-pyropheophorbide dyad, which we obtained for the first time by the Hummelen-Wudl reaction, was chosen as the second dyad. In the present work, a comparative analysis of the influence of the structure of these dyads on their conformation, aggregation properties, absorption spectra, fluorescence, and lifetimes of excited states was carried out for the first time.

Experimental

The synthesis of ***dyad I*** *and its precursors,* methylpyropheophorbide *a* and *d* (Figure 1, compounds **2** and **3**, respectively), as well as methods for its purification and characterization, are described in work.[10]

The synthesis of pyropheophorbide a (Figure 1, compound **4**) was carried out according to the previously described procedure.[22] Product yield: 87.5 %. UV-Vis (C_6H_5N) λ_{max} (relative absorption) nm: 673 (0.4), 613 (0.06), 541 (0.08), 513 (0.07), 417 (1). ^{1}H NMR (500 MHz, $CDCl_3$) δ_H ppm: 9.47 (1H, s, 10-CH), 9.36 (1H, s, 5-CH), 8.55 (1H, s, 20-CH), 7.99 (1H, dd, J = 17.89 Hz, J = 11.58 Hz, 3(1)-CH), 6.27 (1H, d, J = 17.89 Hz, 3(2)-CH *trans*), 6.19 (1H, d, J = 11.58 Hz, 3(2)-CH *cis*), 5.20 (2H, dd, 13(2)-CH_2, J = 19.59 Hz), 4.49 (1H, m, 18-CH), 4.31 (1H, m, 17-CH), 3.65 (2H, q, J = 7.64 Hz, 8(1)-CH_2), 3.58 (3H, s, 12(1)-CH_3), 3.40 (3H, s, 2(1)-CH_3), 3.23 (3H, s, 7(1)-CH_3), 2.68 (2H, m, 17(1)-CH_2), 2.31 (2H, m, 17(2)-CH_2), 1.82 (3H, d, J = 7.3 Hz, 18(1)-CH_3), 1.69 (t, 8(2)-CH_3, J = 7.64 Hz), 0.18 (0.7H, s, 23-NH), –1.67 (0.7H, s, 21-NH).

The synthesis of tosylhydrazone pyropheophorbide a (Figure 1, compound **5**) was carried out by the following procedure: 400 mg (0.75 mmol) of pyropheophorbide *a* and 183 mg (1.5 mmol) of tosylhydrazine were dissolved in 30 mL of isopropanol, 250 μL of concentrated hydrochloric acid was added to the reaction mixture. The reaction mixture was boiled for 10 hours, after which the solvent was removed on a rotary evaporator. Purifica-

tion of the product was carried out chromatographically on silica gel using toluene-isopropanol (1 % vol.) as eluent. Product yield: 234 mg (49 %). UV-Vis (CH_2Cl_2) λ_{max} (relative absorption) nm: 669 (0.34), 610 (0.05), 507 (0.09), 410 (1.00). ^{1}H NMR (500 MHz, $CDCl_3$) δ_H ppm: 9.64 (1H, s, 10-CH), 9.54 (1H, s, 5-CH), 8.73 (1H, s, 20-CH), 8.18 (2H, d, 8.39 Hz, *meta*-Ts), 8.00 (1H, dd, J = 18.13 Hz, J = 11.61 Hz, 3(1)-CH), 7.43 (2H, d, J = 8.39 Hz, *ortho*-Ts), 6.32 (1H, d, J = 18.13 Hz, 3(2)-CH *trans*), 6.16 (1H, d, J = 11.61 Hz, 3(2)-CH *cis*), 5.33 (2H, dd, J = 19.08 Hz, 13(2)-CH_2), 4.59 (1H, m, 18-CH), 4.36 (1H, m, 17-CH), 3.68 (2H, q, J = 7.32 Hz, 8(1)-CH_2), 3.65 (3H, s, 12(1)-CH_3), 3.37 (3H, s, 2(1)-CH_3), 3.28 (3H, s, 7(1)-CH_3), 2.62 (2H, m, 17(1)-CH_2), 2.44 (3H, s, CH_3 Ts), 2.24 (2H, m, 17(2)-CH_2), 1.81 (3H, d, J = 7.03 Hz, 18(2)-CH_3), 1.74 (t, J = 7.40 Hz, 8(2)-CH_3).

The synthesis of ***dyad II*** (Figure 1) was carried out by the Hummelen-Wudl reaction[23] under standard conditions. Tosylhydrazone pyropheophorbide 233.9 mg (0.33 mmol) and 19 mg (0.35 mmol) of sodium methylate were dissolved in 5 mL of dry pyridine in an argon atmosphere. After that, a solution of 1.2 g (1.66 mmol) of fullerene C_{60} in 120 mL of dichlorobenzene was added into the reaction mixture. The obtained reaction mixture was stirred at the boiling temperature for 10 hours. After the reaction completion, the solvent was removed in vacuum, and the product of the reaction was dissolved in pyridine, and the solution was filtered from insoluble impurities. The filtrate was subjected to gel permeation chromatography using cross-linked polystyrene (Bio-Beads S-X1) as the stationary phase and pyridine as eluent. Product yield: 50 mg (12 %). Found: C 89.17, H 3.11, N 5.23 % (calculated for $C_{93}H_{34}N_4O_2 \cdot C_5H_5N$: C 89.28, H 2.98, N 5.31 %). MS (MAI): *m/z* = 1261.251 $[M+Na]^+$, 1277.235 $[M+K]^+$, calculated for $C_{93}H_{34}N_4O_2Na$ 1261.258, $C_{93}H_{34}N_4O_2K$ 1277.232. IR (KBr) ν_{max} cm^{-1}: 3108 w, 2922 m, 2852 m, 1682 s, 1640 w, 1544 w, 1490 w, 1432 m, 1204 s, 1136 m, 838 m, 802 m, 756 m, 724 m, 684 m, 606 m, 520 m, 490 w. UV-Vis (C_6H_5N) λ_{max} (lgε) nm: 673 (3.54), 413 (4.48).

Matrix-activated ionization method (MAI). Mass spectra were acquired using the Exactive Orbitrap high-resolution mass spectrometer (ThermoFisher Scientific, Germany). The sample solutions in the concentrated trifluoroacetic acid were mixed with a saturated solution of the matrix (Phthalonitrile) in acetonitrile in a 1:1 ratio. The concentration of the sample in the prepared solution, according to our estimates, was 5 μM. The sample solution was deposited onto the tip of a stainless-steel wire with a diameter of 0.25 mm by immersing the tip in the solution. The wire was dried at ambient conditions for several seconds after contact with the sample solution, and then the wire was immediately introduced to the inside the mass spectrometer through the inlet capillary of the mass spectrometer inside the mass spectrometric interface with 2 mbar buffer gas pressure. In this region, ions desorbed from the wire were collected by the RF ion funnel and transferred through the skimmer to the mass analyzer. The tip of the wire with the applied solution was located at 10 mm in front of the skimmer. The inner diameter and the temperature of the inlet capillary were 0.6 mm and 25 °C, respectively. The voltages routinely applied to the inlet capillary, the RF ion funnel, and the skimmer of the instrument for ESI mass spectra acquisition were used in these experiments. The resolution of the mass spectrometer was about 10,000. The accuracy of *m/z* values measurement was better than 10 ppm.

Computational simulation of dyads structures. The spatial structures of dyads were geometrically optimized with a semi-empirical quantum chemistry method using the MOPAC2016 package[24] with PM7 and COSMO parameterization methods.[25]

Transient absorption. The previously described pump-probe experimental setup[26] with minor modifications was used. The output of Ti:Sapphire oscillator (800 nm, 80 MHz, 30 fs, "Tsunami", Spectra-Physics, USA) was amplified by a regenerative amplifier ("Spitfire Pro", Spectra-Physics, USA). The repetition rate of the amplified laser pulses was set at 100 Hz. The amplified pulses (800 nm, 100 Hz, 1.5 mJ, 40 fs) were split into two beams. One of the beams was attenuated to 0.8 mJ and directed to a non-collinear optical parametric amplifier ("Topas-white", Light Conversion, Lithuania), the radiation of which was used as a pump pulse. The pump pulse had a Gaussian pulse shape centered at a wavelength of 670 nm, 18 fs duration, and attenuated to 150 nJ pulse energy. The second beam was attenuated to 1 μJ and focused onto the 3 mm quartz cell with pure H_2O to produce a supercontinuum probe pulse. The supercontinuum probe pulse was attenuated and spectrally filtered from excessive radiation in the wavelength range of 780–840 nm and had a smooth spectrum in the wavelength range of 380–900 nm and negligible energy (<10 nJ) to exclude its influence on the observed signal. The pump and probe pulses were delayed relative to each other by a computer-controlled delay line in the range of 0–500 ps, with a resolution from 3.3 fs to 1ps. The pulses were then attenuated, recombined, and focused onto the flow sample cell. The pump and probe light spots had diameters of 200 and 80 μm, respectively. The relative polarizations of pump and probe beams were adjusted to 54.7° (the so-called "magic angle").

The experiments were carried out at 293 K. The circulation rate in the flow cell was 8 mL/min. Pure dry argon was fed into the flow system to avoid contact of the sample solution with air. The supercontinuum probe signal out of the sample was dispersed by a polychromator ("Acton SP-300", Roper Scientific, USA) and detected by CCD camera ("Newton", Andor, USA). Transient absorption spectral changes $\Delta A(t, \lambda)$ were recorded within the range of 380–900 nm.

The measured spectra were corrected for group delay dispersion of the supercontinuum using the procedure described previously.[26,27] The zero time delay between pump and probe pulses was determined in control experiments by recording the signal of a non-resonant coherent burst from pure deaerated pyridine.

Particular attention was paid to the "coherence spike" or "coherent artifact", which is observed at initial delays during the overlap of pump and probe pulses and complicates the analysis of the measurement results at delays < 70 fs. The problem of the resonance signal of a chromophore molecule in the solution for the "coherent spike" time window was analyzed in accordance with work.[28]

Results and Discussion

Synthesis, Separation, and Characterization of Reaction Products

The general scheme of dyads synthesis is shown in Figure 1. The preparation and purification of **dyad I** was carried out according to the methods described in work.[10] **Dyad II** was synthesized by the Hummelen-Wudl reaction[23] under standard conditions. At the same time, in order to avoid the aminolysis of the ester group of methylpyropheophorbide *a* and the formation of tosylhydrazide pyropheophorbide, hydrolysis of the ester group was carried out before the stage of hydrazone formation, with the formation of the free acid of pyropheophorbide. For the purification of **dyad II**, the same technique for the reaction products separation by gel permeation chromatography was used as for **dyad I**,[10] it showed high separation efficiency of the components of the reaction mixture for both dyads.

The **dyad II** had significantly higher solubility in pyridine, compared to the **dyad I**. It was probably because the former dyad has a free carboxyl group, which improves

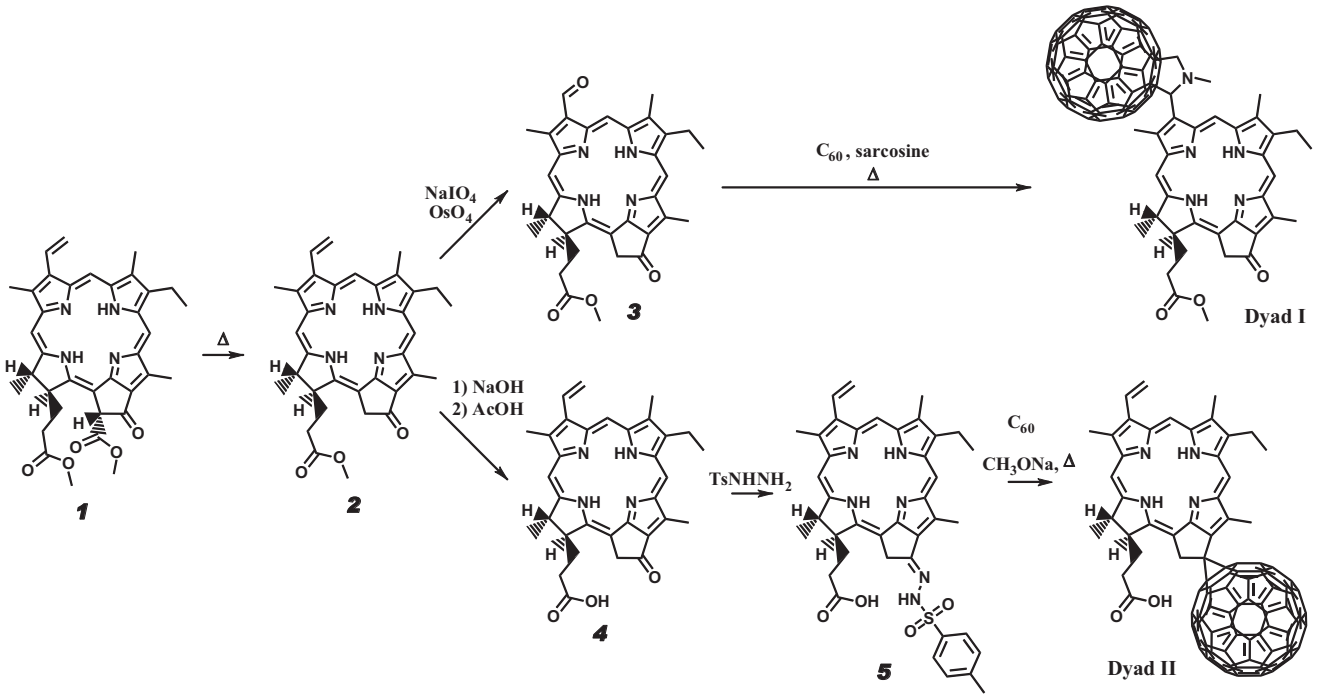

Figure 1. The synthesis scheme of **dyad I** and **dyad II**. The synthesis of **dyad I** and its precursors are described in work.[10]

the interaction with basic solvents and the formation of micellar nanoparticles.

It should be noted that for **dyad II** significantly stronger association processes were observed, which does not allow us to obtain the NMR spectrum for this dyad. The use of different solvents and their mixtures (benzene, carbon disulfide, chloroform, chloroform with the addition of trifluoroacetic acid, DMSO, pyridine with the addition of perfluoropyridine) also did not allow us to obtain the monomeric form of **dyad II** and register its NMR spectrum. Thus, such strong aggregation could not be explained only by hydrophobic interactions. We believe that in this case, exciton and dipole intermolecular interactions play a more significant role, determined by the specific spatial structure **dyad II**, which will be discussed further.

Earlier, we reported that for **dyad I**, the MAI matrix-activated ionization method turned out to be the most effective,[29] which made it possible to record the mass spectra of the dyad itself and the product of double addition of the chlorine residue to fullerene, which could not be done by the APESI and MALDI methods due to fragmentation of their structure. A similar picture was found for **dyad II**: the application of the MALDI method did not give results due to the strong fragmentation of compounds under study, while the use of the MAI method allowed us to reliably record the mass spectrum of the compound (Figure 2A,B). It should be noted that in the case of **dyad II**, it was not protonated molecules of the dyad, but its sodium and potassium adducts (Na^+, K^+), that formed two peaks of molecular ions $[M+Na]^+$ and $[M+K]^+$ (Figure 2), with the practical absence of the peaks $[M+H]^+$ and $[M+2H]^{2+}$, characteristic mass spectra of the **dyad I**.[10] It can be assumed that this is due to the absence of pyrrolidinofullerene nitrogen atom in **dyad II**. Special studies are being carried out to explain the appearance in mass spectra of one or another ion-adduct of chemical compounds.[30] However, the results of these studies are more empirical.

The IR spectra of both pyropheophorbide-fullerene dyads under study had bands, characteristic of pyropheophorbide (about 1544, 1490, 840–680 cm^{-1}), and the fullerene core vibrations (bands 520, 606 and 1432 cm^{-1}). For **dyad II** with a free carboxyl group, an intense band was observed at 1682 and 1204 cm^{-1}, which correspond to this group.

Thus, despite the fact that it was not possible to register NMR spectra of **dyad II**, we think that the combination of applied purification methods and obtained mass-spectra, elemental analysis data, and IR spectra allow us unambiguously confirm the structure of **dyad II**.

Computational Simulation of Dyads Structures

Since the efficiency of electron and the excitation energy transfer processes between fragments of dyads strongly depends on the distance between these fragments, the spatial organization of the obtained dyads is of considerable interest. For the dyads under study, their 3D structure was calculated using the semi-empirical quantum-chemical method PM7[24] in the MOPAC 2016 software package.[25] The resulting models were presented in Figure 3; as can be seen from this figure, the conformations of **dyad I** and **dyad II** had significant differences. In **dyad I**, the dye fragment could be located almost parallel to the tangent plane of the fullerene sphere, which increased the efficiency of the interaction of the π-systems of the dye and fullerene core within the dyad.

On the contrary, for **dyad II**, which had a stiffer cyclopropane linker, the plane of the dye moiety was almost perpendicular to the tangent plane of the fullerene sphere.

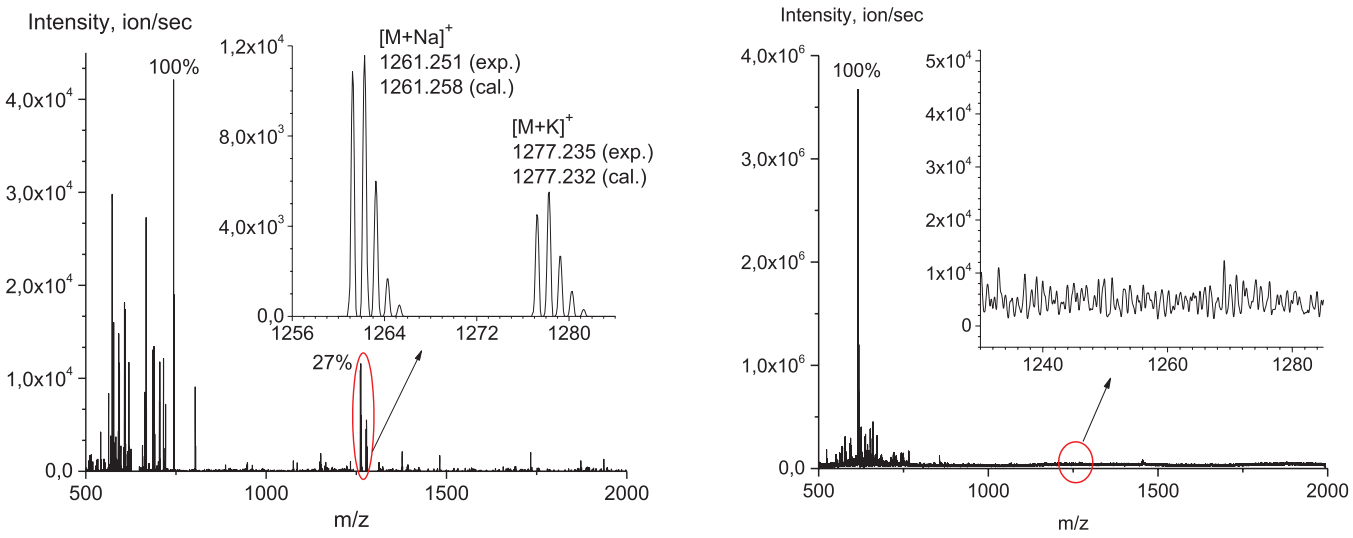

Figure 2. Mass-spectra of **dyad II**: MAI (A) and MALDI (B).

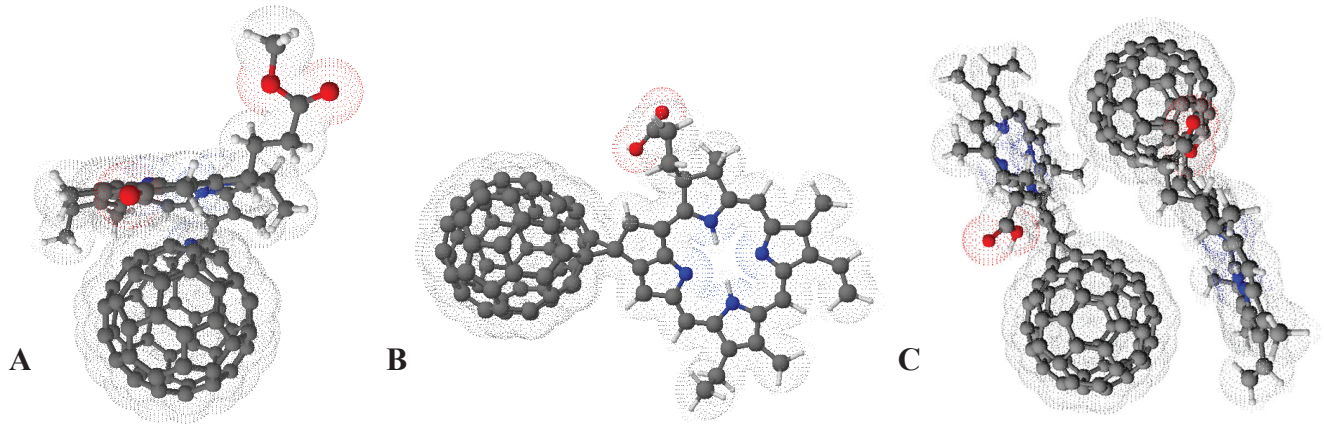

Figure 3. The calculated spatial conformations of **dyad I** (A) and **dyad II** (B), as well as the proposed structure of **dyad II** associates (C).

This configuration could significantly hamper the interaction of π-systems within one dyad, but might enhance intermolecular interactions – such configuration could be convenient for the formation of strong intermolecular π-stacking (Figure 3C), which, we believe, was the reason for the strong aggregation processes, observed for this dyad.

Absorption and Fluorescence Spectra

Upon the analysis of the photophysical properties of dyads, the compound methylpyropheophorbide *a* (**MPP**, Figure 1, compound **2**) was also additionally analyzed as a comparison dye. The absorption spectra of **dyad I** coincide with those presented in work.[10] For this dyad, a weak bathochromic shift of the Soret band (from 417 to 419 nm) and a hypsochromic shift (from 673 to 662 nm) for the *Q*-band peak compared to native dye **MPP** were observed (Figure 4A and Table 1). A similar picture was observed for analogous dyads from work.[20]

In contrast to **dyad I**, the absorption spectrum of **dyad II** in the region of the Soret band was broader and had hypsochromic shift compared to the **MPP** (from 417 to 413 nm), while for the *Q*-band had the only band broadening without a noticeable peak shift (Figure 4A and Table 1). This effect could be caused by strong overlapping of π-orbitals of dye and fullerene systems due to the formation of dyad intermolecular aggregates in a pyridine solution, as it was discussed above.

For **dyad I**, it was not possible to register a fluorescence signal (quenching of fluorescence >5000 times), which was in a good agreement with work.[10] The extremely strong quenching of the fluorescence of this dyad was probably due to its spatial structure, as it was discussed above (Figure 3).

On the contrary, for **dyad II** we were able to record a weak fluorescence signal (quenching by 87 times compared to the native dye **MPP**, Figure 4B and Table 1). For this dyad, one should also note a broadening of the fluorescence spectrum and a hypsochromic shift of its maximum from 676 to 670 nm (Table 1). A similar effect of the fluorescence maximum hypsochromic shift was reported for similar dyads in work.[20] This effect could be explained by the fact that this dyad might form various aggregate types – a smaller amount of a fluorescent aggregate and a large amount of a non-fluorescent aggregate, which could lead to the hypsochromic shift of the maximum of the observed fluorescence signal, as was it shown for other fullerene-chlorin dyads in work.[9]

Table 1. Photophysical properties of fullerene-pyropheophorbide dyads (solvent – pyridine).

Property \ Compound	**MPP**	**dyad I**	**dyad II**
Absorbance at Soret band peak (λ_{Dmax}), nm	417	419	413
Absorbance at *Q*-band peak (λ_{Dmax}), nm	673	662	673
Fluorescence peak (λ_{FLmax}), nm	676	–	670
Relative fluorescence quantum yield*	0.026	–	< 0.001
Fluorescence quenching compared to the free dye **MPP**, fold	1	> 5000	87
The calculated distance between the dye and the fullerene core centers, Å	–	6.54	10.2
Excited state lifetimes τ, ps; and their fractional intensities (*A*, %)	–	τ_1 = 20; (A_1 = 100)	τ_1 = 0.40 ± 0.008; (A_1 = 61) τ_2 = 12 ± 0.3; (A_2 = 22) τ_3 = 100 ± 1.8; (A_3 = 17)

*It was calculated by the method[31] using fluorescein as a reference compound.

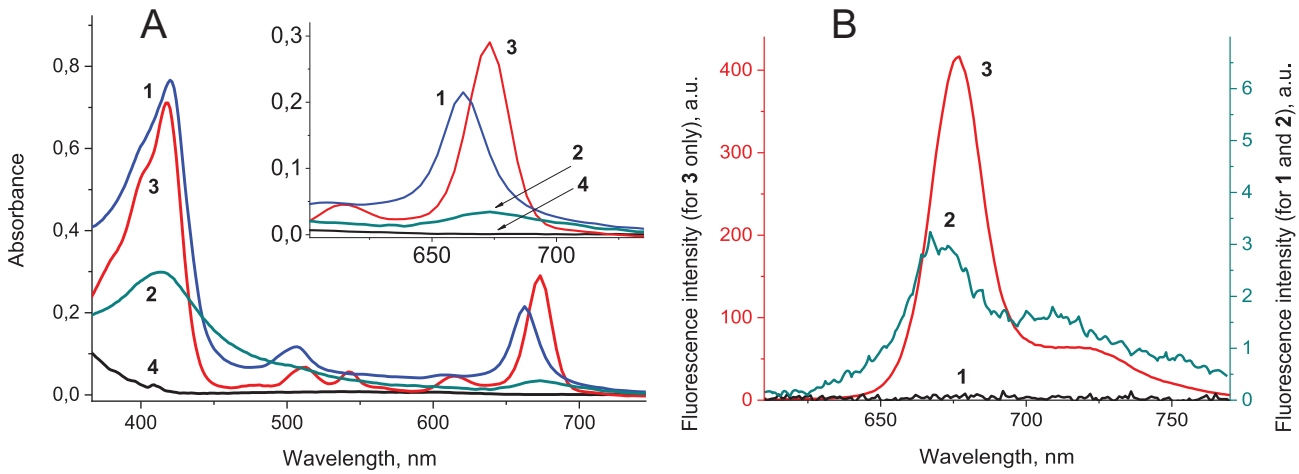

Figure 4. Absorption spectra (A) and fluorescence (B) spectra: **dyad I** (1), **dyad II** (2), native dye **MPP** (3) and native fullerene C_{60} (4) (fluorescence not shown). All compounds were dissolved in pyridine at a concentration of 10 μM. For fluorescence λ_{ex} = 417 nm.

Transient Absorption Measurements

Time-resolved transition absorption spectroscopy was performed for both dyads with 670 nm excitation wavelength in pyridine solution. For **dyad I**, a reasonable standard deviation was obtained already by monoexponential approximation of the obtained kinetic data; more complex two- and three-exponential data approximations did not lead to a decrease in the standard deviation. The time constant of the relaxation process was ~20 ps (Figure 5A, and Table 1), which was close to the 26 ps value, previously reported for this dyad[19] as the excimer state relaxation time. This relaxation pattern was in good agreement with the absence of a fluorescence signal for this dyad (Figure 6). More complex three- and four-exponential relaxation models, which were reported for the same dyad in earlier studies[19] were probably associated with the presence of fluorescent impurities, the purification of which by sorption chromatography is practically impossible.[10]

For **dyad II**, a more complex relaxation pattern was observed. The smallest standard deviation was achieved using a three-exponential model. The time constants were 0.40±0.008 ps, 12±0.3 ps, and 100±1.8 ps (Figure 5B,D, and Table 1). The process corresponding to a time constant of 0.4 ps can be attributed to the short-lived components of the fluorescence decay, or ultrafast internal conversion (Figure 6). Approximately 61 % of the excited molecules relax by this pathway. A time constant of 12 ps correlates well with intermolecular relaxation processes; this relaxation path brings another 22 % of the excited molecules to the ground state. Such large value also indicates strong association processes of **dyad II** in pyridine solution. The time constant of 100 ps could be attributed to the relaxation process of the excimer state; the weight contribution of this process was about 17 %.

The slower excimers relaxation kinetics for **dyad II**, compared to **dyad I**, as well as the lower efficiency of its formation, could be explained by their different spatial conformation. **Dyad I** had an optimal configuration

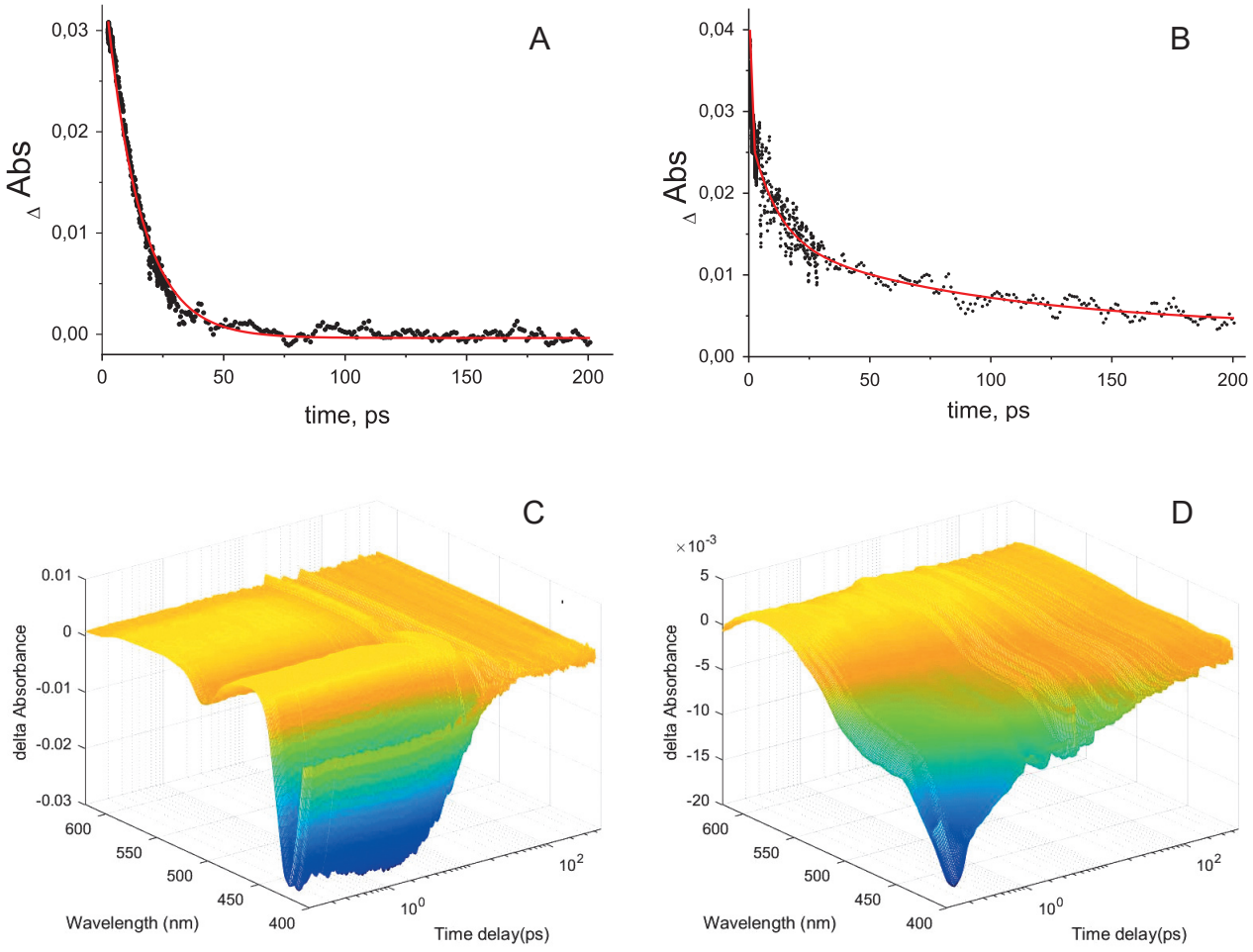

Figure 5. Time-resolved transient absorption curves of dyads: **dyad I** (A) and **dyad II** (B). The solid lines correspond to the global fittings. The initial transient absorption spectra of dyads are also shown: **dyad I** (C) and **dyad II** (D). Dyads were dissolved in pyridine; all spectra of samples were recorded after excitation by a 25-fs laser pulse at 670 nm.

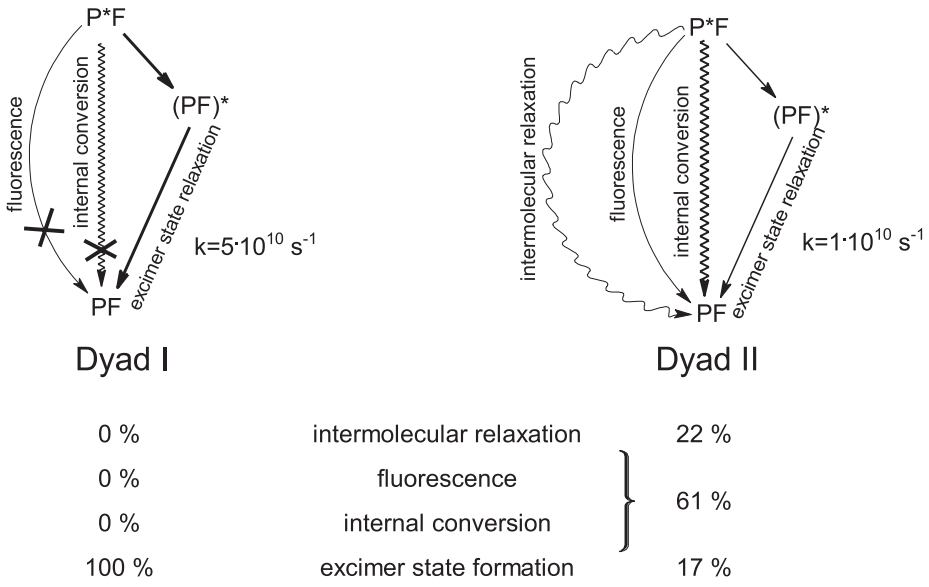

Figure 6. Transient states and possible excited state relaxation pathways of dyads under study.

for electron transfer between dye and fullerene π-systems and a minimum distance in the molecule, which leads to the effective formation of fullerene-dye excimers, and also to rapid relaxation of this state. For **dyad II**, a change in the relative location of dye and fullerene moieties led to an increase in the distance between dyad fragments (Table 1) and to a decrease in the electron transfer efficiency between these fragments. It was manifested in the appearance of a fluorescence signal for **dyad II**, in the decrease of excimer relaxation rate and, consequently, in the significant decrease of the electron transfer process contribution to the excited state relaxation of the dye moiety of the dyad.

A similar picture of the excited states lifetimes is described for analogous fullerene-porphyrin and fullerene-chlorin systems, and the obtained excimer state lifetimes for the studied dyads (20–100 ps) turned out to be one of the shortest for such systems.[20,32] Apparently, this is due both to the short linker length between the fullerene core and the dye, and, in the case of **dyad I**, also to the orientation of the dye relative to the fullerene core that is optimal for excimer formation. Another factor that could further reduce the of the dyad excimer state lifetime – is the type of solvent (pyridine); solvents with relatively low polarity could hamper the formation of excimer or charge transfer states.

Conclusion

Thus, we developed a new approach to the synthesis of the fullerene-pyropheophorbide dyad based on the Hummelen-Wudl reaction (**dyad II**). For this dyad and the previously obtained **dyad I**, a comparative analysis of the influence of the mutual arrangement of the π-aromatic systems of the dye and the fullerene core on the physicochemical properties of the studied dyads was carried out. **Dyad I** had a "parallel" spatial conformation that ensures the predominance of the intramolecular interaction of the dye and fullerene moieties. This dyad was characterized by the dominant decay path of the excited state through the excimer state. On the contrary, **dyad II** "perpendicular" spatial conformation enhanced the intermolecular interaction, and the decay of the excited state through excimers was significantly suppressed by other relaxation paths.

Thus, upon the change of the location of the dye and fullerene moieties relative to each other, due to the various conformations, it was possible to significantly affect both the efficiency of the interaction of dye and fullerene moieties and the aggregation properties of dyads, which, in turn, determined the nature and relaxation times of dyad excited states.

The obtained data are important for the further development of directional design methods of photoactive fullerene-dye dyads as new highly effective photosensitizers for photodynamic therapy.

Acknowledgements. The transient absorption measurements of dyads were performed using the facilities of Semenov FRCCP RAS CCE (N 506694). The synthesis of dyads and the analysis of their photophysical properties were funded by the Russian Science Foundation (project N 18-74-00128). The analysis of dyads by MAI method was supported by the Program of Basic Researches for Russian State Academies of Sciences 2013-2020 (state registration N AAAA-A18-118112690060-9).

References

1. Lebedeva V.S., Mironova N.A., Ruziev R.D., Mironov A.F. *Macroheterocycles* **2019**, *11*, 339.
2. Bertran J.C., Montforts F.-P. *Eur. J. Org. Chem.* **2017**, *2017*, 1608.
3. Wang S., Duan S., Wang Y., Sun C., Wang X.-F., Sasaki S. *J. Energy Chem.* **2019**, *38*, 88.
4. Nikkonen T., Oliva M.M., Kahnt A., Muuronen M., Helaja J., Guldi D.M. *Chem. – A Eur. J.* **2015**, *21*, 590.
5. Kavakka J.S., Heikkinen S., Kilpeläinen I., Tkachenko N.V., Helaja J. *Chem. Commun.* **2009**, 758.
6. Ballatore M.B., Spesia M.B., Milanesio M.E., Durantini E.N. *Eur. J. Med. Chem.* **2014**, *83*, 685.
7. Li Q., Huang C., Liu L., Hu R., Qu J. *Cytometry Part A* **2018** *93*, 997.
8. Hamblin M.R. *Photochem. Photobiol. Sci.* **2018**, *17*, 1515.
9. Rybkin A.Y., Belik A.Y., Goryachev N.S., Mikhaylov P.A., Kraevaya O.A., Filatova N.V., Parkhomenko I.I., Peregudov A.S., Terent'ev A.A., Larkina E.A., Mironov A.F., Troshin P.A., Kotelnikov A.I. *Dyes Pigm.* **2020**, *180*, 108411.
10. Rybkin A.Y., Belik A.Y., Tarakanov P.A., Taziev K.R., Kozlov A.V., Goryachev N.S., Sulimenkov I.V., Kozlovskiy V.I., Romanenko Y.V., Koifman O.I., Kotelnikov A.I. *Macroheterocycles* **2019**, *12*, 181.
11. Belik A.Y., Mikhailov P.A., Kraevaya O.A., Rybkin A.Y., Khakina E.A., Goryachev N.S., Usol'tseva L.I., Romanenko Y.V., Koifman O.I., Gushchina O.I., Mironov A.F., Troshin P.A., Kotel'nikov A.I. *Dokl. Phys. Chem.* **2017**, *477*, 222.
12. He D., Du X., Xiao Z., Ding L. *Org. Lett.* **2014**, *16*, 612.
13. Kang H., Cho C.H., Cho H.H., Kang T.E., Kim H.J., Kim K.H., Yoon S.C., Kim B.J. *ACS Appl. Mater. Interfaces* **2012**, *4*, 110.
14. Liu C., Xu L., Chi D., Li Y., Liu H., Wang J. *ACS Appl. Mater. Interfaces* **2013**, *5*, 1061.
15. Yoon S.C., Nam S.Y., Lee C., Kang H., Kim B.J., Kim P.S., Kim K.-H., Cho C.-H., Jung J. *Chem. Mater.* **2011**, *23*, 5090.
16. Han G.D., Collins W.R., Andrew T.L., Bulović V., Swager T.M. *Adv. Funct. Mater.* **2013**, *23*, 3061.
17. Prat F., Stackow R., Bernstein R., Qian W., Rubin Y., Foote C.S. *J. Phys. Chem. A* **1999**, *103*, 7230.
18. Kordatos K., Ros T. Da, Prato M., Leach S., Land E.J., Bensasson R.V. *Chem. Phys. Lett.* **2001**, *334*, 221.
19. Tkachenko N.V., Rantala L., Tauber A.Y., Helaja J., Hynninen P.H., Lemmetyinen H. *J. Am. Chem. Soc.* **1999**, *121*, 9378.
20. Vehmanen V., Tkachenko N.V., Tauber A.Y., Hynninen P.H., Lemmetyinen H. *Chem. Phys. Lett.* **2001**, *345*, 213.
21. Efimov A., Tkatchenko N.V., Vainiotalo P., Lemmetyinen H. *J. Porphyrins Phthalocyanines* **2001**, *5*, 835.
22. Uliana M.P., Pires L., Pratavieira S., Brocksom T.J., de Oliveira K.T., Bagnato V.S., Kurachi C. *Photochem. Photobiol. Sci.* **2014**, *13*, 1137.
23. Hummelen J.C., Knight B.W., LePeq F., Wudl F., Yao J., Wilkins C.L. *J. Org. Chem.* **1995**, *60*, 532.
24. Stewart J.J.P. *MOPAC2016. Version: 16.353W* **2016**.
25. Stewart J.J.P. *J. Mol. Model.* **2013**, *19*, 1.
26. Shelaev I.V., Gostev F.E., Vishnev M.I., Shkuropatov A.Y., Ptushenko V.V., Mamedov M.D., Sarkisov O.M., Nadto-

chenko V.A., Semenov A.Y., Shuvalov V.A. *J. Photochem. Photobiol. B: Biology* **2011**, *104*, 44.
27. Kovalenko S.A., Dobryakov A.L., Ruthmann J., Ernsting N.P. *Phys. Rev. A* **1999**, *59*, 2369.
28. Dobryakov A.L., Pérez Lustres J.L., Kovalenko S.A., Ernsting N.P. *Chem. Phys.* **2008**, *347*, 127.
29. Trimpin S. *J. Am. Soc. Mass Spectrom.* **2016**, *27*, 4.
30. Kruve A., Kaupmees K. *J. Am. Soc. Mass Spectrom.* **2017**, *28*, 887.
31. Rurack K. In: *Standardization and Quality Assurance in Fluorescence Measurements I*. Springer Berlin Heidelberg, **2008**. p. 101.
32. Guldi D.M. *Chem. Soc. Rev.* **2002**, *31*, 22.

Received 04.05.2020
Accepted 09.06.2020